

Strong Absorption Model Analysis for ^{12}C Ion Elastic Scattering at $E_{lab}=420$ MeV

Yong Joo Kim and Dong Shik Kang
Department of Physics, Cheju National University, Cheju 690-756
(August, 1998)

A phase shift analysis of elastic scattering angular distributions for ^{12}C scattering on ^{12}C and ^{40}Ca targets at $E_{lab}=420$ MeV is presented using the Ericson strong absorption model. The calculated results reproduced fairly well the observed data. A near- and far-side decomposition following the Fuller's formalism is performed. Also, the optical potentials by inversion are calculated and compared with the optical model results.

PACS numbers (s) :25

I. INTRODUCTION

In recent year, there have been a great deal efforts in describing elastic and inelastic scattering process within the framework of the Ericson strong absorption model (SAM) [1]- [6]. It is known that this simple model could provides a good description of nucleus-nucleus and hadron-nucleus scattering data over a large energies range. Phase shift analysis based on the McIntyre SAM [7] and Ericson SAM have been applied to the elastic scattering data of $^{12}\text{C} + ^{12}\text{C}$ system and ^{16}O scattering on ^{12}C , ^{40}Ca , ^{90}Zr and ^{208}Pb target nuclei [2]. Recently, Choudhury [5] analyzed elastic scattering data of 800 MeV/c charged kaons from ^{12}C and ^{40}Ca nuclei using a phenomenological model which is based on Ericson strong absorption model. This phenomenological model, although macroscopic in character, is found to be an excellent representation of the microscopic theory.

Recently, there are several attempts to evaluate optical potential from parametrized phase shift. Woods-Saxon type model potentials with the parameters that can be determined directly from the McIntyre parametrization of the phase shift, for heavy-ion collision, were obtained from solving the inversion problem [8] And, Eldebawi *et al.* [6] use the simple Ericson parametrization of the phase shifts to analyze the experimental data and apply the Glauber approximation to evaluate the corresponding optical potential. Sahm *et al.* [9] have observed the elastic scattering angular distributions for ^{12}C on ^{12}C , ^{40}Ca , ^{90}Zr and ^{208}Pb at $E_{lab} = 420$ MeV and have analyzed these data using optical model fits with Woods-Saxon potentials.

In the previous papers [10]- [12], a semiclassical phase shift analysis based on McIntyre SAM [7] was presented. It was applied satisfactorily to the so-called Fresnel pattern $^{12}\text{C} + ^{90}\text{Zr}$ and $^{12}\text{C} + ^{208}\text{Pb}$ systems at $E_{lab}/A = 35$ MeV/nucleon. In this paper, we present a phase shift analysis of the elastic scattering data [9] for $E_{lab} = 420$ MeV ^{12}C beams on ^{12}C and ^{40}Ca target nuclei based on Ericson SAM instead of McIntyre SAM. The near-side and far-side decomposition of the elastic cross section due to the Fuller's relationship [13] will be presented. Also,

we will calculate the optical potentials by the inversion and compare them with the optical model analysis results [9]. Section II, we present the scattering amplitude and potential by inversion. Finally, results and conclusions are presented in section III.

II. SCATTERING AMPLITUDE AND POTENTIAL BY INVERSION

The elastic differential scattering cross section is given by the following equation:

$$\frac{d\sigma}{d\Omega} = |f(\theta)|^2 \quad (1)$$

but in case of symmetry system for spinless particles, such as $^{12}\text{C} + ^{12}\text{C}$, by the following formula:

$$\frac{d\sigma}{d\Omega} = |f(\theta) + f(\pi - \theta)|^2. \quad (2)$$

Where the elastic scattering amplitude for spin-zero particle via Coulomb and short-range central force is given by

$$f(\theta) = f_R(\theta) + \frac{1}{ik} \sum_{l=0}^{\infty} \left(l + \frac{1}{2}\right) \times \exp(2i\sigma_l) (S_l^N - 1) P_l(\cos \theta). \quad (3)$$

Here $f_R(\theta)$ is the usual Rutherford scattering amplitude, $\sigma_l = \arg \Gamma(l + 1 + i\eta)$ the Coulomb phase shifts and S_l^N denotes the nuclear scattering matrix written by

$$S_l^N = \exp(2i\delta_l) = A_l \exp(2i\delta_l^R). \quad (4)$$

In this work, we use the Ericson parametrization of the S-matrix. The parametrized S-matrix suggested by Ericson is given by [1]

$$S_l^N = \{1 + \exp(-\mu - i\alpha)\}^{-1} \quad (5)$$

where $\mu = (l - l_g)/\Delta$. This equation can be rewritten as

$$S_l^N = \{1 + 2 \cos \alpha e^{-\mu} + e^{-2\mu}\}^{-1} e^{2i\delta_l^R} \quad (6)$$

with

$$\delta_l^R = \frac{1}{2} \arctan\left[\frac{\sin \alpha}{\cos \alpha + e^\mu}\right]. \quad (7)$$

The reduced radius $r_{1/2}$ and diffusivity d are related to the grazing angular momentum l_g and angular momentum width Δ through the following semi-classical relationship [2]:

$$l_g = kR_{1/2}\left(1 - \frac{2\eta}{kR_{1/2}}\right)^{1/2} \quad (8)$$

$$\Delta = kd\left(1 - \frac{\eta}{kR_{1/2}}\right)\left(1 - \frac{2\eta}{kR_{1/2}}\right)^{-1/2}. \quad (9)$$

where $R_{1/2} = r_{1/2}(A_1^{1/3} + A_2^{1/3})$, k is the wave number and $\eta = mZ_1Z_2e^2/(\hbar^2k)$ the Sommerfeld parameter.

The nuclear phase shift can be rewritten as

$$\delta_l = \frac{i}{2} \ln\left|1 + \exp\left(\frac{b_0 - b - i\rho}{a}\right)\right|. \quad (10)$$

where b and b_0 are the impact parameters normally given by $kb = l + \frac{1}{2}$, $kb_0 = l_g + \frac{1}{2}$, $k\rho = \alpha\Delta$ and a is diffusivity with $a = \frac{\Delta}{k}$. Using the relation between nuclear phase shift and optical potential

$$\delta(b) = -\frac{1}{\hbar v} \int_b^\infty \frac{V(r)}{\sqrt{r^2 - b^2}} r dr. \quad (11)$$

Eq.(11) is of Abel's type and the inversion solution of these equations are given by [6]

$$V(r) = \frac{2\hbar v}{\pi} \frac{1}{r} \frac{d}{dr} \int_r^\infty \frac{\delta_l(b)}{\sqrt{b^2 - r^2}} b db. \quad (12)$$

Replacing $b = \sqrt{r^2 + u^2}$, we can derived the following optical potential form

$$V(r) = \frac{\hbar v}{\pi a i} \int_0^\infty du \frac{1}{\sqrt{r^2 + u^2}} \times \left[1 + \exp\left(\frac{\sqrt{r^2 + u^2} - b_0 + i\rho}{a}\right)\right]^{-1}. \quad (13)$$

The integration in Eq.(13) can be calculated numerically using the parameters of Ericson phase shift.

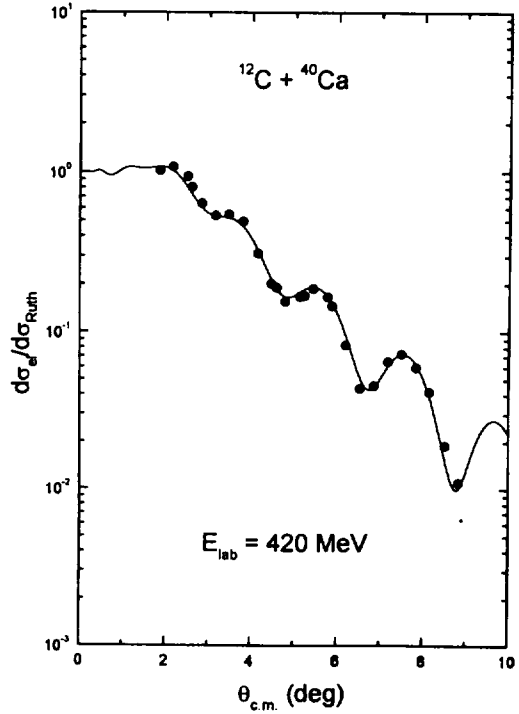
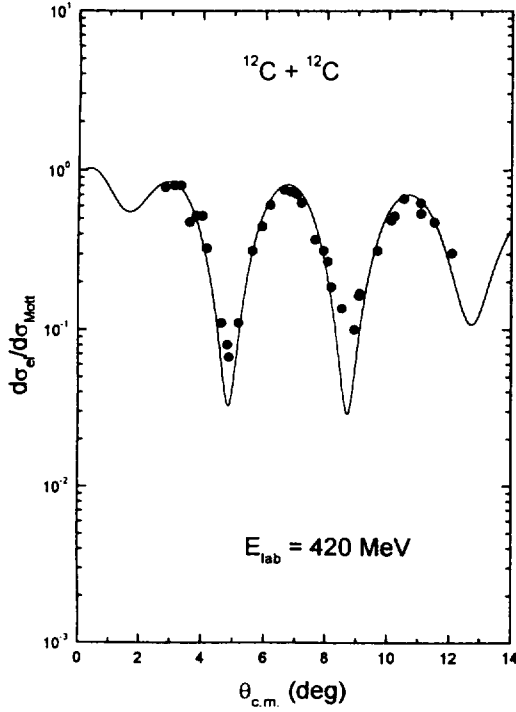


Figure 1: Elastic scattering angular distributions for $^{12}\text{C} + ^{12}\text{C}$ and $^{12}\text{C} + ^{40}\text{Ca}$ systems at $E_{\text{lab}} = 420$ MeV. The solid circles denote the observed data taken from Sahn *et al.* [9]. The solid curves are the calculated results from the Ericson strong absorption model.

III. RESULTS AND CONCLUSIONS

The elastic differential cross sections are obtained by using partial wave sum, Eq.(1)-Eq.(3) and Ericson phase shifts, Eq.(6) and Eq.(7). The numerical results for $^{12}\text{C} + ^{12}\text{C}$ and $^{12}\text{C} + ^{40}\text{Ca}$ systems at $E_{\text{lab}} = 420$ MeV are presented in Fig.1. The fits are satisfactorily and the corresponding parameters are given in Table 1. The parameters were determined by least square fits. It can be noticed in table 1 that the two grazing angular momenta, l_g s, and the corresponding widths, Δ s, increase as the target masses increase. Total cross section σ_R in this Ericson SAM lead to fairly good agreement with those of an optical model analysis [9], and increase as the target masses increase as expected. We can see also in this ta-

ble that the strong absorption radius $R_{1/2}$, for which $T(R_{1/2}) = \frac{1}{2}$, provides a proper estimation of the reaction cross section in terms of $\sigma'_R = \pi R_{1/2}^2$: $\sigma'_R = 1151$ mb for $^{12}\text{C} + ^{12}\text{C}$ and 1864 mb for $^{12}\text{C} + ^{40}\text{Ca}$.

The deflection functions θ_l given by the formula, $\theta_l = 2 \frac{d}{dl}(\sigma_l + \delta_l^R)$, are plotted in Fig.2 along with the corresponding transmission function T_l , $T_l = 1 - |S_l^N|^2$, for the elastic scatterings of $^{12}\text{C} + ^{12}\text{C}$ and $^{12}\text{C} + ^{40}\text{Ca}$ at $E_{\text{lab}} = 420$ MeV. The deflection functions are calculated from an equation

$$\theta_l = 2 \arctan\left(\frac{\eta}{l}\right) - \frac{1}{\Delta} \frac{\sin \alpha \exp(-\mu)}{1 + 2 \cos \alpha \exp(-\mu) + \exp(-2\mu)} \quad (14)$$

Table 1. Ericson's phase shift analysis for ^{12}C beams at $E_{\text{lab}} = 420$ MeV.

Target	$r_{1/2}(fm)$	$d(fm)$	α	l_g	Δ	$l_{1/2}$	$\theta_{N.R.}^{(0)}$	$\sigma_R^{SAM}(mb)$	$\sigma_R^{OM}(mb)^a$
^{12}C	1.273	0.663	1.529	44.289	5.149	47	-2.85	1203	1259
^{40}Ca	1.286	0.804	1.360	84.449	9.611	92	1.86	1961	1989

^a Values of the optical model analysis are taken from Sahn *et al.* [9].

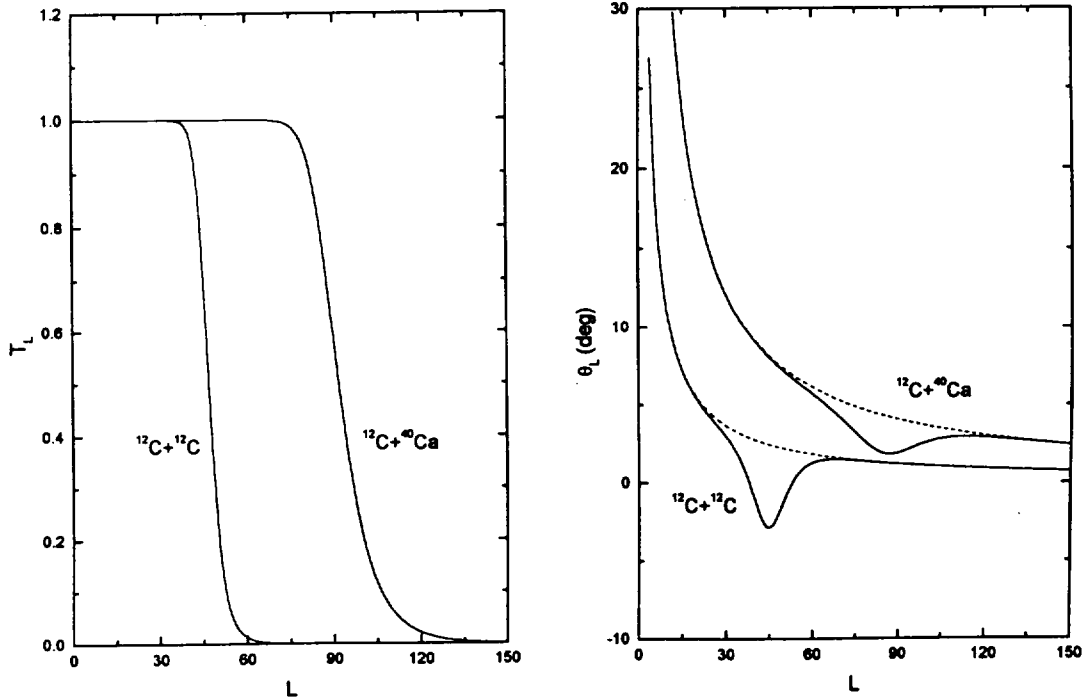


Figure 2: Transmission functions and deflection functions for $^{12}\text{C} + ^{12}\text{C}$ and $^{12}\text{C} + ^{40}\text{Ca}$ systems in the Ericson strong absorption model plotted against the angular momentum L . The dashed curves indicate the deflections for the Coulomb phase shifts only. The solid curves denote the deflection functions for the Coulomb plus nuclear phase shifts

where $\mu = (l - l_g)/\Delta$.

It can be noticed that a presence of a nuclear rainbow is clearly evidenced in both case. In this figure, we can also find that transmission functions and the deflection functions are shifted to larger angular momenta as the target masses increase. Such a shifts raise the values of critical angular momentum $l_{1/2}$ corresponding to the strong absorption radius $R_{1/2}$, for which $T(R_{1/2}) = \frac{1}{2}$.

The near- and far-side decompositions of the scattering amplitude with the Ericson parametrization of S-matrix were also performed by following the Fuller's formalism [13]. The contributions of the near- and far-side components to elastic scattering cross sections are shown in Fig.3 along with the total differential cross section. The total differential cross section is not just a sum of the near- and far-side cross sections but contains the interference between near- and far-side amplitudes as seen in Fig.3. The refraction oscillation observed on the elastic scattering cross section of the $^{12}\text{C} + ^{12}\text{C}$ system is due to the strong interference between the near-side and far-side component as seen in Fig.3. The magnitudes of the near- and far-side contributions are about the same around 6.5° ; however, the far-side dominates at angles greater than this angle. On the other hand, in the case

of $^{12}\text{C} + ^{40}\text{Ca}$ elastic scattering, the far-side component becomes very small compared to the near-side one over the whole range of angles. Because of the smallness of the far-side amplitude, we can see that the cross section of the $^{12}\text{C} + ^{40}\text{Ca}$ system show weak Fraunhofer oscillations.

The comparison of the real and imaginary parts of optical potential with those of Woods-Saxon potentials obtained in optical model analysis [9] and the potentials previously deduced using Ericson SAM is shown in Fig.4. Using our fitting parameter for l_g, Δ and calculating other parameters (such as η, k , etc.), we got the phase shift parameters as b_0 and a . Note that Coulomb effects have been subtracted off in evaluating the parameters cited above. The potentials obtained in the present paper agree with those obtained in Woods-Saxon potentials by optical model analysis near the strong absorption radius. This can only be understood by recognizing the strong absorption nature of reactions under consideration, which renders the scattering insensitive to the value of the potential at small impact parameter.

In this paper, we have shown that it is possible to give a satisfactory account of the elastic scatterings of $E_{\text{lab}} = 420$ MeV ^{12}C ions from ^{12}C and ^{40}Ca within the Ericson

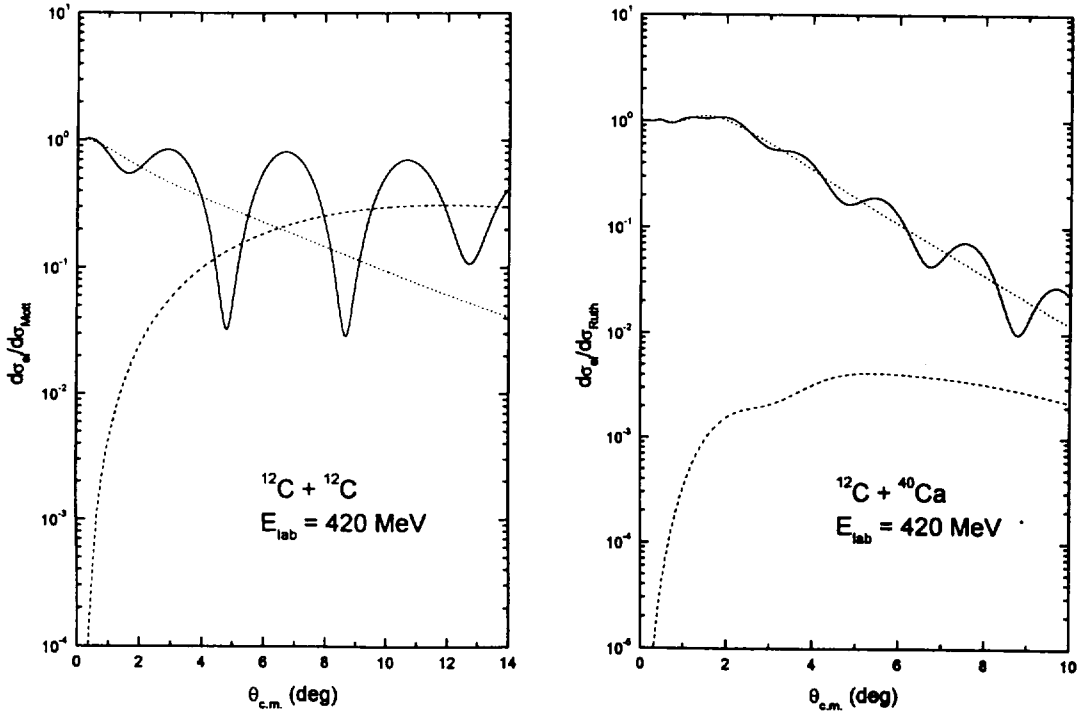


Figure 3: Differential cross sections (solid curves), near-side contributions (dotted curves), and far-side contributions (dashed curves) of the $^{12}\text{C} + ^{12}\text{C}$ and $^{12}\text{C} + ^{40}\text{Ca}$ elastic scattering angular distribution following the Fuller's formalism[13] by using Ericson parametrization of S-matrix.

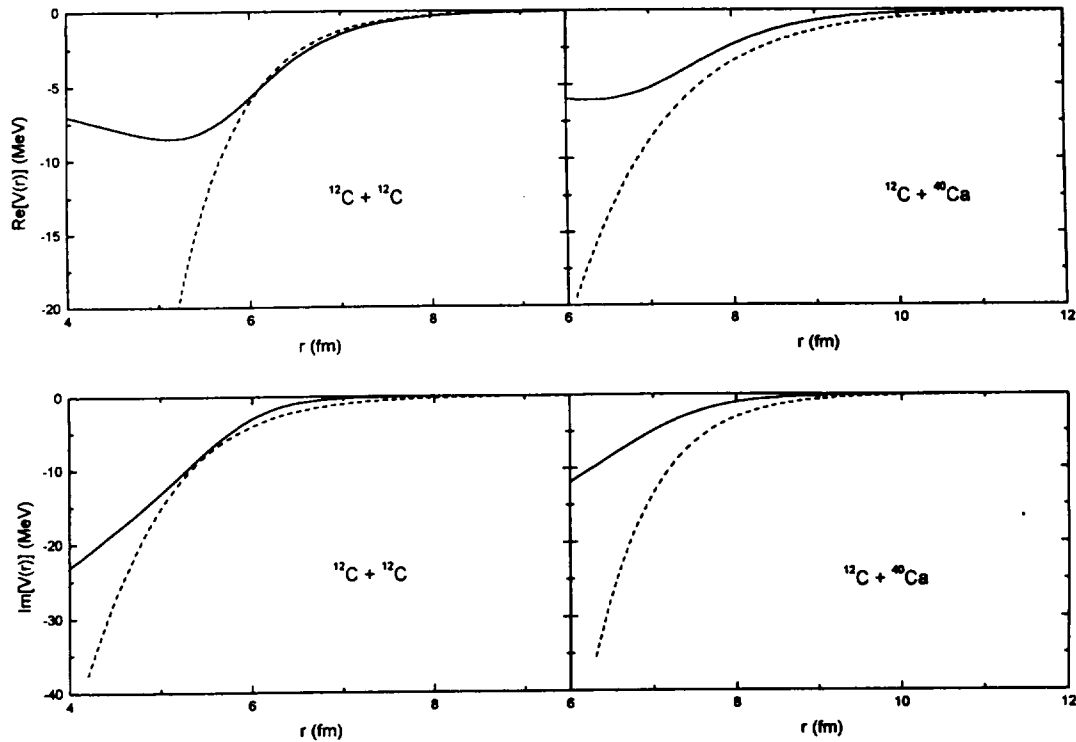


Figure 4: The real($\text{Re}[V(r)]$) and imaginary parts($\text{Im}[V(r)]$) of the optical potential for $^{12}\text{C} + ^{12}\text{C}$ and $^{12}\text{C} + ^{40}\text{Ca}$ elastic scattering at 420 MeV. The solid lines are the calculated results in the Ericson strong absorption model. The dashed lines are the calculated from the optical model analysis taken from Ref.[9].

SAM. We can see that the presence of nuclear rainbow is also evidenced by the deflection functions. Through a near-side and far-side decomposition of the cross section, we have shown that the refraction oscillations of the $^{12}\text{C} + ^{12}\text{C}$ system are due to the strong interference between the near-side and far-side amplitude, and the near-side one dominates for the $^{12}\text{C} + ^{40}\text{Ca}$ system. We can find that potentials obtained from inversion procedure agree with phenomenological Woods-Saxon potentials from the optical model analysis near the strong absorption radius.

- [1] W. E. Frahn, *Diffraction Processes in Nuclear Physics* (Oxford Press, Oxford, 1985).
 [2] M. C. Mermaz, *Z. Phys.* **A321**, 613 (1985).

- [3] D. C. Choudhury and T. Guo, *Phys. Rev.* **C39**, 1883 (1989).
 [4] D. C. Choudhury and M. A. Scura, *Phys. Rev.* **C50**, 979 (1994).
 [5] D. C. Choudhury, *J. Phys.* **G22**, 1069 (1996).
 [6] N. M. Eldebawi and M. H. Simbel, *Phys. Rev.* **C53**, 2973 (1996).
 [7] J. A. McIntyre, K. H. Wang and L. C. Becker, *Phys. Rev.* **117**, 1337 (1960).
 [8] H. M. Fayyad and T. H. Rihan, *Phys. Rev.* **C53**, 2334 (1996).
 [9] C. C. Sahm *et al.*, *Phys. Rev.* **C34**, 2165 (1986).
 [10] M. H. Cha and Y. J. Kim, *J. Phys. G: Nucl. Part. Phys.* **16**, L281 (1990).
 [11] M. H. Cha, B. K. Lee, K. S. Sim and Y. J. Kim, *J. Korean Phys. Soc.* **23**, 450 (1990).
 [12] M. H. Cha, B. K. Lee and Y. J. Kim, *J. Korean Phys. Soc.* **23**, 369 (1990).
 [13] R. C. Fuller, *Phys. Rev.* **C12**, 1561 (1975).